Doppler shift of a laser pulse beam scattered by a rotating cone and cylinder*

Wang Bao-Ping(王保平)[a], Wang Ming-Jun(王明军)[b]†, Wu Zhen-Sen(吴振森)[c], Li Ying-Le(李应乐)[b], and Xiang Ning-Jing(向宁静)[b][c]

[a] *National Key Laboratory of Sciences and Technology on UAV, Northwestern Polytechnical University, Xi'an* 710072, *China*
[b] *School of Physics and Electronic Engineering, Xianyang Normal College, Xianyang* 712000, *China*
[c] *School of Science, Xidian University, Xi'an* 710071, *China*

(Received 16 July 2013; revised manuscript received 7 October 2013; published online 25 March 2014)

Based on laser radar equations, a Doppler shift model of a laser pulse beam scattered by a rotating arbitrary convex target is reported in this paper. The boundary relations between an incident pulse beam and the detected area elements are analyzed by geometric methods. The Doppler shift characteristics of the rotating cone and cylinder are discussed and the difference between the laser pulse beam and the plane wave scattered from the same rotating target is compared accordingly. Numerical simulations show that the Doppler shift is tightly relevant to their dimensions, speeds, and so on. In the same incidence conditions, the pulse beam and plane wave have difference peak values and the same Doppler shift bandwidth. If the waist radius of the pulse beam is larger, the peak value is higher, and the Doppler shifts are proportional to the speed of the rotating target. By virtue of our theoretical model, we probe into the scattered characteristics of the Doppler shifts of a laser pulse beam, which would benefit target identification in national defense.

Keywords: scattered characteristics of laser pulse beams, Doppler shift, laser radar, target identification

PACS: 03.65.Nk, 42.55.Ah, 42.25.Kb, 41.20.–q **DOI:** 10.1088/1674-1056/23/5/050303

1. Introduction

Lasers can be distinguished from other light sources by their coherence, which enables them to be ubiquitous and have various applications in the modern world, especially in the fields of aerospace, national contravallation, and the military.[1–7] With the development of laser detection technologies, the scattered characteristics of laser beams from targets with a rough surface has been an increasingly interesting research subject. To boost the laser radar imaging technology, there is an urgent need of relevant theories and the experiments in the past several decades.[8–17] In the early period, the plane wave was replaced by the incidence laser in theoretical detection models.[18,19] The Kirchhoff approximation method has been used to discuss the scattered cross sections for arbitrarily shaped dielectric objects with rough surfaces in the optical and infrared laser frequencies.[20,21] However, according to the electromagnetic theory, a laser light is described as a Gaussian beam.[22] Some researchers have investigated the scattered characteristics of Gaussian beams from dielectric and conducting targets.[23–26] In recent years, the rapid development of laser detection technologies has created a great demand for theoretical models. As a result, the pulse beam, as the closest theoretical model of the laser, has been brought forward in order to obtain more precise models in Lidar engineering applications. For the pulse beams scattered by a static target, we have derived equations to describe the light scattering of a rigid body,[27,28] and carried out laser high-range resolution profile (LHRRP) simulations.[29]

It is very significant to study the motions of rough targets such as ballistic missiles, namely, translation, rotation, and vibration. In theoretical and experimental work, laser Doppler velocimetric techniques have been used to determine the velocity of large-sized rough targets as well as the angular velocity of rotating surfaces.[30] Bankman used a plane wave as the incident laser to present an analytical model of Doppler spectra in the backscatter from cones and cylinders rotating around their axes, and compared the model spectra of a cone with the observed experimental spectra in Ref. [31]. In Ref. [32], when a plane wave was used as an incident laser, the Doppler spectra of rotating convex bodies such as superspheroids, superspheroid cylinders, and their combinations of cylinders and cones have been reported.

Based on the above research background, we build a more desired model to further study the Doppler shift characteristics by replacing a plane wave with a pulse beam.

*Project supported by the National Natural Science Foundation of China (Grant Nos. 61271110, 60801047, and 61073106), the New Scientific and Technological Star Project of Shaanxi Province, China (Grant No. 2011KJXX39), the Aviation Science Foundation (Grant No. 2011ZC53042), and the Natural Science Foundation of Shaanxi Province, China (Grant Nos. 12Jk0955 and 2014JQ0816).

†Corresponding author. E-mail: wmjxd@aliyun.com

© 2014 Chinese Physical Society and IOP Publishing Ltd

2. The Doppler shift model of a laser pulse beam scattered by a rotating convex target

2.1. Scattering theory: laser radar equation

As the laser is scattered from the target by using models of the plane wave, the laser radar equation reads[15,33]

$$P_{\rm s} = \frac{P_{\rm i}}{4\pi r_{\rm r}^2}\frac{\sigma}{4\pi r_{\rm r}^2}\frac{\pi D^2}{4}\eta_{\rm Atm}\eta_{\rm Sys}, \tag{1}$$

where $P_{\rm s}$ is the received backscattered power, $P_{\rm i}$ is the transmitter laser power, σ is the effective target scattering cross section, $r_{\rm r}$ is the distance between the target center and the transmit-receive system, D is the receiver aperture diameter, $\eta_{\rm Atm}$ is the attenuation factor of the atmosphere, and $\eta_{\rm Sys}$ is the system efficiency. Using the Gaussian beam, the amplitude of the incidence laser can be written as[34]

$$u(\boldsymbol{r}', z) = E_0\frac{\omega_0}{\phi(z)}\exp\left[-\frac{g_0(\boldsymbol{r}')}{\phi(z)^2}\right], \tag{2}$$

where ω_0 is the waist radius, $\phi(z)$ is the beam radius, $\boldsymbol{r}'$ is the position between the point of the target and the target center, and $g_0(\boldsymbol{r}')$ is the square of the distance between any point of the target and the band center axis. According to the scattering theory of rough surfaces, Eqs. (1) and (2), Cheng and Wang presented the laser radar equations of a pulse beam, which have been continuously revised in Refs. [27] and [28]. The power $P_{\rm s}(t)$ of the pulse beam scattered by the unit area $\Delta A_{\rm s}$ of the target are given by

$$\begin{aligned}\Delta P_{\rm s}(t) &= \frac{P_{\rm i}T_{\rm A1}\eta_{\rm t}}{4\pi\phi^2\rho_0^2}w_0^2\exp\left[-\frac{2g_0(\boldsymbol{r}')}{\phi^2\rho_0^2}\right]\\ &\quad\times\sigma(\boldsymbol{r}')\frac{T_{\rm A2}}{4\pi\rho_0^2}\frac{\pi D^2\eta_{\rm r}}{4}\Delta A_{\rm s}.\end{aligned} \tag{3}$$

From Eq. (3), the backward power $P_{\rm s}(t)$ of the pulse beam scattered by the target is expressed as

$$\begin{aligned}P_{\rm s}(t) &= \int {\rm d}S'\,\frac{P_{\rm i}T_{\rm A1}\eta_{\rm t}}{4\pi\phi^2\rho_0^2}\pi w_0^2\exp\left[-\frac{2g_0(\boldsymbol{r}')}{\phi^2\rho_0^2}\right]\\ &\quad\times\sigma(\boldsymbol{r}')\frac{T_{\rm A2}}{4\pi\rho_0^2}\frac{\pi D^2\eta_{\rm r}}{4},\end{aligned} \tag{4}$$

where $P_{\rm s}(t)$ is the including coherent, $P_{\rm c}(t)$ and incoherent $P_{\rm f}(t)$, the laser radar equation of a pulse beam scattered by an arbitrary convex target can be expressed as

$$P_{\rm s}(t) = P_{\rm c}(t) + P_{\rm f}(t), \tag{5}$$

$$\begin{aligned}P_{\rm c}(t) &= \frac{k_0^2w_0^4\sigma_{\rm g}}{64\pi\rho_0^4}|R(0)|^2|\chi(-2k_0)|^2\exp\left[-\frac{k_0^2w_0^2g_0(\boldsymbol{r}_0')}{2\rho_0^2}\right]\\ &\quad\times P_{\rm i}(t-2\rho_0/c+2\boldsymbol{k}_{\rm s}\cdot\boldsymbol{r}_0'/c),\end{aligned} \tag{6}$$

$$\begin{aligned}P_{\rm f}(t) &= \frac{k_0^2w_0^4}{64\pi\rho_0^4}\int {\rm d}S'\exp\left[-\frac{k_0^2w_0^2g_0(\boldsymbol{r}_0')}{2\rho_0^2}\right]\\ &\quad\times\sigma_{\rm p}^0(\boldsymbol{r}')P_{\rm i}(t-2\rho_0/c+2\boldsymbol{k}_{\rm s}\cdot\boldsymbol{r}_0'/c),\end{aligned} \tag{7}$$

where $\phi = 2/k_0w_0$, ϕ is the width of the pulse, ρ_0 is the detected distance, and w_0 is the beam waist radius, and $\sigma(\boldsymbol{r}')$ is the pulse beam scattered cross section which includes two parts: coherent $\sigma_{\rm c}^0(\boldsymbol{r}')$ and incoherent $\sigma_{\rm p}^0(\boldsymbol{r}')$ scattered section. D is the aperture of detector, $T_{\rm A1}$ and $T_{\rm A2}$ are the rates of the average atmospheric transmission, and $\eta_{\rm t}$ and $\eta_{\rm r}$ are the optical efficiency of the emission and receiver system

2.2. The Doppler shift model of a laser pulse beam scattered by an arbitrary rotating convex target

In order to discuss the Doppler characteristics, we make two assumptions: (i) the target rotates around its fixed axis, (ii) the laser pulse beam incident the convex targets, which means there is no secondary and multi-scattered from their surface. The coordinate system of the laser pulse beam scattered from an arbitrary convex target is shown in Fig. 1. In this target coordinate system, the origin is located in the centroid of the target, the target rotating around the z axis with angular velocity ω, incidence optical power $P_{\rm i}$, and the incidence and detector are in the same direction $\boldsymbol{n}_2$, $\Delta A_{\rm s}$ is the scattered area element, β is the angle between the area element normal $\boldsymbol{n}_1$ and $\boldsymbol{n}_2$, α is the angle between the instantaneous velocity detector v and $\boldsymbol{n}_2$, and the received optical power on the surface area elements $\Delta A_{\rm s}$ is given by Eq. (3). From the relationship between the bidirectional reflectance distribution function $f_{\rm r}$ and per unit area of laser radar cross section $\sigma(\boldsymbol{r}')$[33]

$$\sigma(\boldsymbol{r}') = 4\pi f_{\rm r}\cos\theta_{\rm i}\cos\theta_{\rm s}, \tag{8}$$

where $\theta_{\rm i}$ and $\theta_{\rm s}$ are respectively the incident and scattered angle under the backward scattered condition.

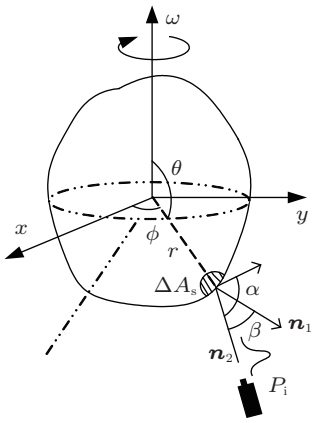


Fig. 1. Coordinate relations of laser pulse beam scattered from a rotating arbitrary convex target.

We put Eq. (8) into Eq. (3) and obtain

$$\begin{aligned}\Delta P_{\rm s} &= \frac{P_{\rm i}T_{\rm A1}\eta_{\rm t}}{\pi\phi^2\rho_0^2}\pi w_0^2\exp\left[-\frac{2g_0(\boldsymbol{r}')}{\phi^2\rho_0^2}\right]\\ &\quad\times\frac{T_{\rm A2}}{4\pi\rho_0^2}\frac{\pi D^2\eta_{\rm r}}{4}\Delta A_{\rm s}4\pi f_{\rm r}\cos\theta_{\rm i}\cos\theta_{\rm s}.\end{aligned} \tag{9}$$

In the target coordinates, let us suppose that the surface of the target will satisfy

$$f(r\sin\theta\cos\phi, r\sin\theta\sin\phi, r\cos\phi) = 0. \tag{10}$$

From Fig. 1, as the target rotates around the z axis, the surface element of the Doppler frequency shift is given by

$$\Delta f = \frac{2\omega r\cos\theta\cos\alpha}{\lambda}, \tag{11}$$

where λ is the laser wavelength, and r is the position vector of the scattering surface element. From the above equations, x and Δf satisfy the following relationship:

$$x = \pm\frac{\lambda\Delta f}{2\omega\sin\lambda}. \tag{12}$$

The area element normal $\boldsymbol{n}_1$ will be expressed as

$$\boldsymbol{n}_1 = \frac{1}{(f_x^2+f_y^2+f_z^2)^{1/2}}(f_x, f_y, f_z), \tag{13}$$

where $f_x = \partial f(x,y,z)/\partial x$, $f_y = \partial f(x,y,z)/\partial y$, and $f_z = \partial f(x,y,z)/\partial z$. According to differential relations, ΔA_s and Δx, Δz satisfy $\Delta A_s = \Delta x\Delta z/\cos\eta$, η is the angle between the surface normal $\boldsymbol{n}_1$ and the y axis. It is defined as

$$g(x,z) = \frac{1}{|\cos\eta|} = \left|\frac{(f_x^2+f_y^2+f_z^2)^{1/2}}{f_y}\right|. \tag{14}$$

Then the laser radar equation of a pulse beam scattered by arbitrary scattered targets will be given by

$$\begin{aligned}\Delta P_s = {} & \frac{P_i T_{A1}\eta_t}{\pi\phi^2\rho_0^2}\pi w_0^2\exp\left[-\frac{2g_0(\boldsymbol{r}')}{\phi^2\rho_0^2}\right] \\ & \times\frac{T_{A2}}{4\pi\rho_0^2}\frac{\pi D^2\eta_r}{4}\left|\frac{(f_x^2+f_y^2+f_z^2)^{1/2}}{f_y}\right| \\ & \times 4\pi f_r\cos\theta_i\cos\theta_s\Delta x\Delta z.\end{aligned} \tag{15}$$

3. The Doppler shift of a rotating cone and cylinder

From the scattered equation (13) of a laser pulse beam, we choose the rotating cone and cylinder and build their Doppler shift models. For the cone, it rotates within the yz plane, r_b is the cone radius, γ is the angle between the cone rotating axis and the z axis, α is the half cone angle, and the incident laser pulse beam is parallel to the z axis. The relationship between the coordinate systems are shown in Fig. 2. The conical surface satisfies the following function:

$$x^2 + y^2 = (z\tan\alpha + c)^2, \tag{16}$$

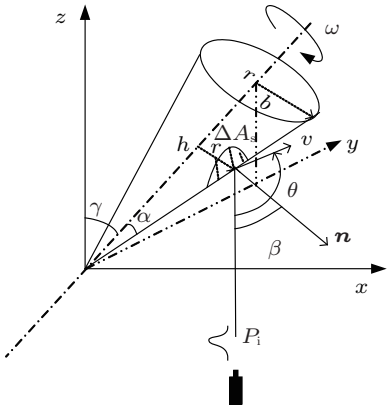


Fig. 2. Laser pulse beam scattered from a rotating cone.

The arbitrary scattered area element ΔA_s will be given by $\Delta A_s = \Delta x\Delta z/\cos\eta$. The geometric and the light illuminated effects of a rotating cone are shown in Fig. 3. From the relationship between the geometry and the coordinate, the function $g(x,z)$ will be expressed as

$$g(x,z) = \frac{1}{|\cos\eta|} = \left|\frac{z\sin\alpha\cos\alpha\cos\gamma \pm \sin\gamma\sin\alpha\sqrt{x^2(\sin^2\alpha-\cos^2\gamma)+z^2\sin^2\alpha}}{\cos\alpha(\sin^2\alpha-\cos^2\gamma)\sqrt{x^2(\sin^2\alpha-\cos^2\gamma)+z^2\sin^2\alpha}}\right|. \tag{17}$$

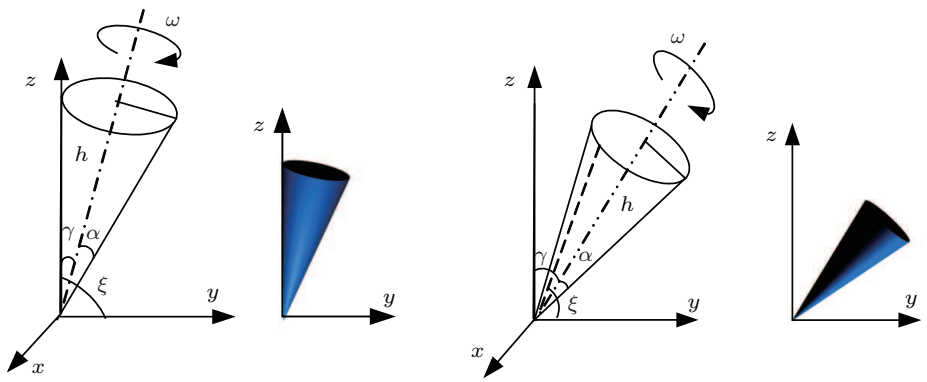


Fig. 3. (color online) Coordinate and angle relations and scattered area of the effective model for a rotating cone.

If the surface of the cone is illuminated by a laser pulse beam, the area will depend on two boundary conditions. The first boundary condition requires that the coordinate z will be changed in the following range:

$$0 < z < \frac{h}{\cos\gamma} - y\tan\gamma. \tag{18}$$

The second boundary condition is $\cos\beta \le 0$. Considering the scattered area element ΔA_s, rotating radial r and incidence angle β will be expressed by

$$\begin{aligned} r &= \sqrt{x^2 + (y\cos\gamma - z\sin\gamma)}, \\ \cos\beta &= \frac{x\sin\gamma}{\sqrt{x^2 + (y\cos\gamma - z\sin\gamma)}}. \end{aligned} \tag{19}$$

Doppler shift spectra Δf and x are satisfied with Eq. (10). According to Eq. (13), the laser radar equation of pulse beam scattered from an arbitrary scattered target will be given by

$$\begin{aligned} \Delta P(x,z) &= \frac{P_i T_{A1}\eta_t}{4\pi\phi^2\rho_0^2}\pi\exp\left[-\frac{2g_0(\boldsymbol{r}')}{\phi^2\rho_0^2}\right]\frac{T_{A2}}{4\pi\rho_0^2} \\ &\quad\times\frac{\pi D^2\eta_r}{4}\Delta A f(\beta)\,|\cos\beta| \\ &= \frac{P_i T_{A1}\eta_t}{4\pi\phi^2\rho_0^2}\pi\exp\left[-\frac{2g_0(\boldsymbol{r}')}{\phi^2\rho_0^2}\right]\frac{T_{A2}}{4\pi\rho_0^2} \\ &\quad\times\frac{\pi D^2\eta_r}{4}\frac{\Delta x\Delta z}{|\cos\xi|}\rho(\pi-\beta)\,|\cos\beta|, \end{aligned} \tag{20}$$

where ξ is the angle between the illuminated region edge and the z axis. The geometry and coordinate of the laser pulse beam scattered area of a rotating cone target are shown in Fig. 3.

$$|\cos\xi| = \frac{\sin\gamma\sqrt{(z\tan\alpha + c)^2 - x^2}}{|z\tan\alpha + c|\sqrt{1+\tan^2\alpha}}. \tag{21}$$

According to the scattered area condition $\cos\beta < 0$,

$$\begin{aligned} &\cos\beta \\ &= \frac{\pm\sin\gamma\sqrt{(z\tan\alpha + c)^2 - x^2} - (z\tan\alpha + c)\tan\alpha\cos\gamma}{|z\tan\alpha + c|\sqrt{1+\tan^2\alpha}} \\ &< 0. \end{aligned} \tag{22}$$

Substituting Eqs. (19) and (20) into Eq. (18) yields

$$\begin{aligned} &\Delta P(x,z) \\ &= \frac{P_i T_{A1}\eta_t}{\pi\phi^2\rho_0^2}\pi\exp\left[-\frac{2g_0(r')}{\phi^2\rho_0^2}\right]\frac{T_{A2}}{4\pi\rho_0^2}\frac{\pi D^2\eta_r}{4}\Delta x\Delta z\rho(\pi-\beta) \\ &\quad\times\frac{\left|\pm\sin\gamma\sqrt{(z\tan\alpha + c)^2 - x^2} - (z\tan\alpha + c)\tan\alpha\cos\gamma\right|}{\sin\gamma\sqrt{(z\tan\alpha + c)^2 - x^2}}. \end{aligned} \tag{23}$$

In the case of the rotating cylinder, from Eq. (14), that is, $\tan\alpha = 0$, which are given as the cylinder surface, are satisfied in the following relationship $x^2 + y^2 = c^2$.

In this case, the incidence angle $\cos\beta$ is given by

$$\cos\beta = \frac{\pm\sin\gamma\sqrt{c^2 - x^2}}{c} < 0. \tag{24}$$

The range of the angle γ from 0 to π, the geometric and the light illuminated effects of a rotating cylinder are shown in Fig. 4. The coordinate argument z will be changed in the following range:

$$-y\tan\gamma < z < -y\tan\gamma + \frac{h}{\cos\gamma}. \tag{25}$$

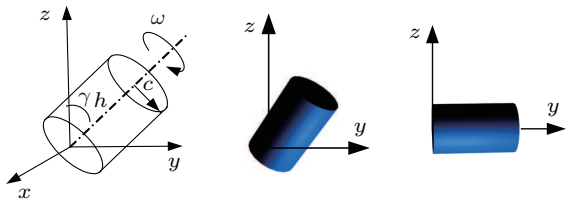


Fig. 4. (color online) Coordinate and angle relations and scattered area of the effective model for a rotating cylinder.

From Eqs. (13) and (18), the Doppler shift of a laser pulse beam scattered by a rotating cylinder is given by

$$\begin{aligned} \Delta P(x,z) &= \frac{P_i T_{A1}\eta_t}{\pi\phi^2\rho_0^2}\pi\exp\left[-\frac{2g_0(r')}{\phi^2\rho_0^2}\right]\frac{T_{A2}}{4\pi\rho_0^2}\frac{\pi D^2\eta_r}{4} \\ &\quad\times\Delta x\Delta z\rho(\pi-\beta)\left|\frac{\pm\sin\gamma\sqrt{c^2 - x^2}}{c}\right|. \end{aligned} \tag{26}$$

4. Comparison of the Doppler shift between a laser pulse beam and a plane wave scattered by a rotating cone and cylinder

In this section, utilizing Eqs. (18)–(25), we simulate the Doppler spectra of a pulse beam scattered by a rotating cone and cylinder with an incidence laser wavelength $\lambda = 1.06$ μm, a numerical step of $\Delta x = 5$ mm, and $\Delta z = 10$ μm. The plane wave calculations and pulse beam results are compared in a different geometry and rotational speed of cylindrical and conical target Doppler shift characteristics. The numerical results are shown in Figs. 5 and 6.

For the rotating cone, the half angle $\alpha = 5.7°$, $11.3°$, $h = 1$ m the rotating speed $\omega = 1$ rad/s, 2rad/s. From Figs. 5(a) and 5(c), the rotating speed is faster, and the Doppler shift is higher in the same half angle and height. From Figs. 5(b) and 5(c), the radius is greater, and the Doppler shift is also higher in the same rotating speed and height.

For the rotating cylinder, the radius $c = 1$, 2 m, $h = 1$ m, and rotating speed $\omega = 1$, 2 rad/s. From Figs. 6(a) and 6(c), the Doppler shift distribution of the cylinder is the same as the cone, that is, the Doppler shift is proportional to the radius of the cylinder at the same rotational speed. At the same time, if the cylinders have the same radii, the Doppler shift is proportional to the rotating speed.

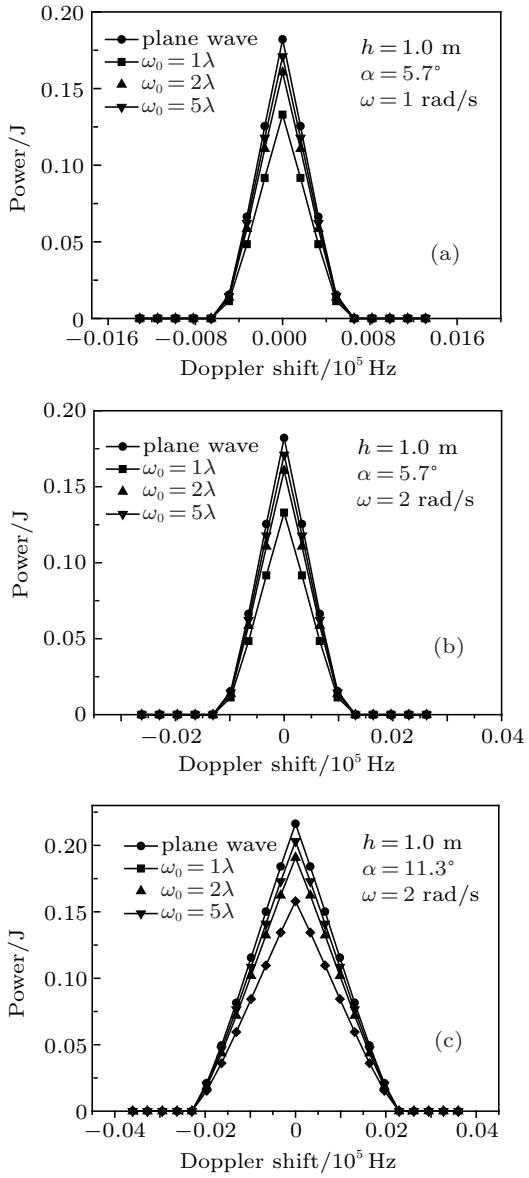


Fig. 5. The Doppler shift of the rotating cone compared the pulse beam with plane wave.

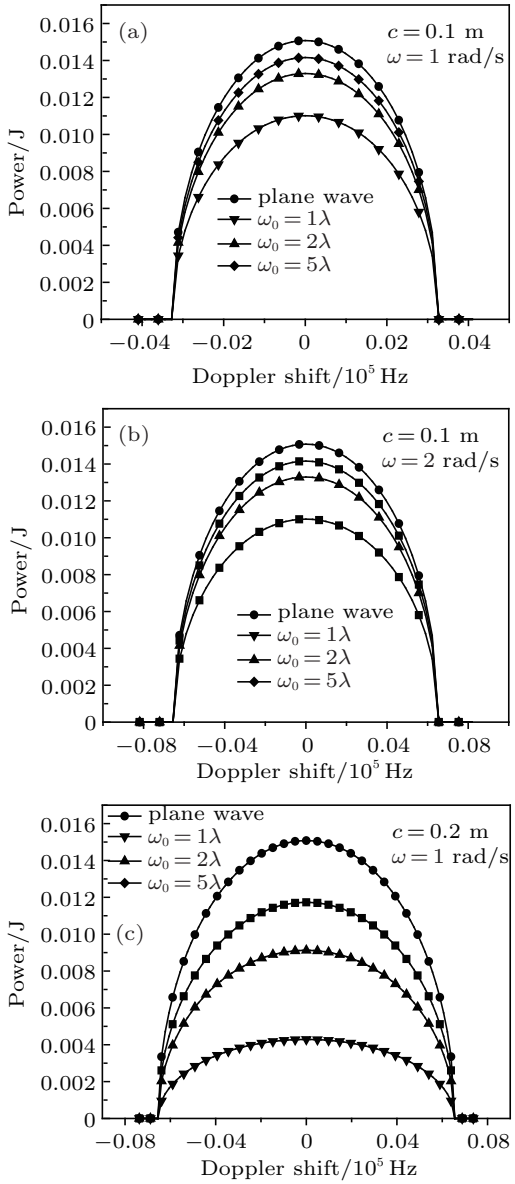


Fig. 6. The Doppler shift of the rotating cylinder compared the pulse beam with plane wave.

Figures 5 and 6 also show that the Doppler shift characteristics of detected powers are affected by the waist radius of the incidence laser pulse beam. It is found that the greater the waist radius is, the higher the probe power will be.

As the same waist radius of the incidence laser pulse beam, their laser Doppler shift is proportional to the target rotating speed. For the rotating cylinder and cone target, in the same rotating speed, the Doppler spectrum shift is proportional to their dimensions in height and radius.

5. Conclusions

Based on the pulse beam scattered from an arbitrary target of the rough target, we built a theoretical model to investigate the Doppler shift of a rotating arbitrary target. As an important special case, we choose the rotating cone and cylinder, and discuss their characteristics of Doppler shift. We find out the difference between a laser pulse beam and a plane wave scattered by the same rotating target. Numerical simulations show that the Doppler shift is tightly relevant to the dimensions, speeds, pulse width, and so on. We present the scattering characteristics of the Doppler shift of the laser pulse beam, which enables a refined theoretical model to study the micromotion of missiles, and will build a research foundation for further study of laser detecting targets. Our results could play an important role in target identification in national defense.

References

[1] Schultz K I and Fisher S 1992 *Appl. Opt.* **31** 7690
[2] Mullen L J, Vieira A J, Herezfeld P R and Contarino V M 1995 *IEEE Trans.* **43** 2370
[3] Verly J G and Delanoy R L 1996 *Proc. IEEE* **84** 126
[4] Aniceto B and Barry J R 2000 *Appl. Opt.* **39** 2401
[5] Schultz K and Fisher S 1992 *AIAA* **92** 1365
[6] Jacques G V and Delanoy R L 1996 *Proc. IEEE* **84** 126

[7] Yan Z G, Bian B M, Wang S Y, Lin Y L, Wang C Y and Li Z H 2013 *Chin. Phys. B* **22** 060505
[8] Jelalian A V 1980 *Electronics and Aerospace Systems Conference* 546
[9] Obert L B and Charles E B 1987 *Opt. Lett.* **12** 239
[10] Jeffrey H S 1982 *Appl. Opt.* **2** 3398
[11] Andrews Aaron Keith 1994 *Computer and Optical Simulation of Radar* Imaging Systems (PhD thesis) (Washington: Washington State University)
[12] Vaughhan J M, Steinvall K O, Werner C and Flamant P 1996 *Proc. IEEE* **84** 205
[13] Alfred B G and William E K 2000 *Lincoln Laboratory Journal* **12** 383
[14] Dai Y J 2002 *Principles of Laser Radar* (Beijing: National Defence Industry Press) (in Chinese)
[15] Gregory O 2002 *Optical Detection Theory for Laser Applications* (NewYork: John Wiley and Sons)
[16] Wei H Y, Wu Z S and Peng H 2008 *Acta Phys. Sin.* **57** 6666 (in Chinese)
[17] Dang W J, Zeng X D and Feng Z J 2013 *Acta Phys. Sin.* **62** 024204 (in Chinese)
[18] Ogilvy J A 1991 *Theory of Wave Scattering from Random Rough Surfaces* (Bristol: Taylor and Francis Ltd)
[19] Ishimaru A 1978 *Wave Propagation and Scattering in Random Media* (New York: Academic Press)
[20] Wu Z S and Cui S M 1992 *Inter. J. Infrared Mill. Waves* **13** 537
[21] Bruce N C 1995 *Appl. Opt.* **34** 5531
[22] Dawis L W 1979 *Phys. Rev. A* **19** 1177
[23] Collin R E 1994 *IEEE Trans. Antennas Propagat.* **42** 70
[24] Wang M J, Wu Z S and Li Y L 2008 *Prog. Electromagn. Res. B* **4** 223
[25] Li H Y, Wu Z S and Li Z J 2010 *Chin. Phys. B* **19** 104202
[26] Lian T H, Wang S Y and Guo Z 2011 *Acta Phys. Sin.* **60** 124208 (in Chinese)
[27] Chen H 2004 *Scattering of Gaussian Beam by Object with Rough Surface and its Application on Laser One-Dimensional Range Profile* (PhD thesis) (Xi'an: Xidian University) (in Chinese)
[28] Wang M J 2008 *Research on Scattering of Pulse Beam by Target with Rough Surface and its Laser Range Doppler Imaging* (PhD thesis) (Xi'an: Xidian University) (in Chinese)
[29] Wang M J, Wu Z S, Li Y L and Zhang G 2009 *Prog. Electromagn. Res.* **96** 193
[30] Gong Y J, Wu Z S and Wu J J 2010 *Chin. Phys. Lett.* **26** 024213
[31] Bankman 2000 *J. Opt. Soc. Am. A* **17** 465
[32] Gong Y J, Wu Z S and Wang M J 2010 *Opt. Laser. Eng.* **48** 107
[33] Ulaby F T, Moore R K and Fung A K 1982 *Microwave Remote Sensing* (Boston: Addison-Wesley Publishing Company)
[34] Lü B D 2003 *Laser Optic: Beam Characterization, Propagation and Tranformation Resonator Technology and Physics* (Beijing: Higher Education Press) (in Chinese)